

Determination of the Electronical Bandstructure by Angle Resolved Photoemission

Research Seminar Surface Physics

Matthias Kreier

Humboldt Universität zu Berlin
Arbeitsgruppe Elektronische Eigenschaften und Supraleitung

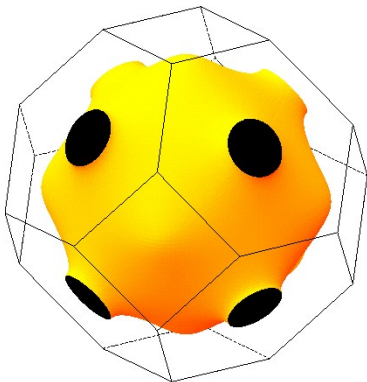
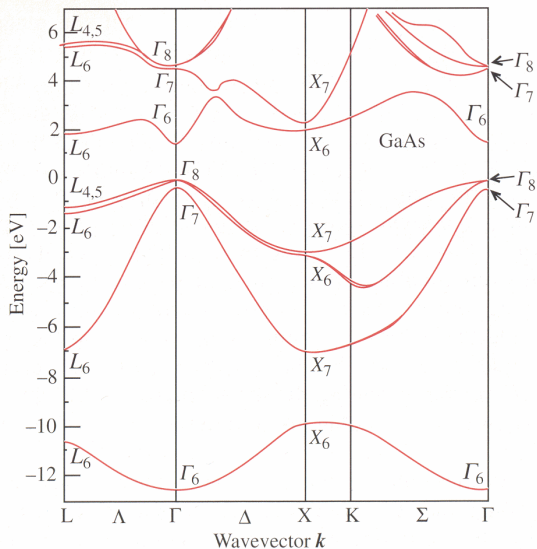
14. 5. 2007



Overview

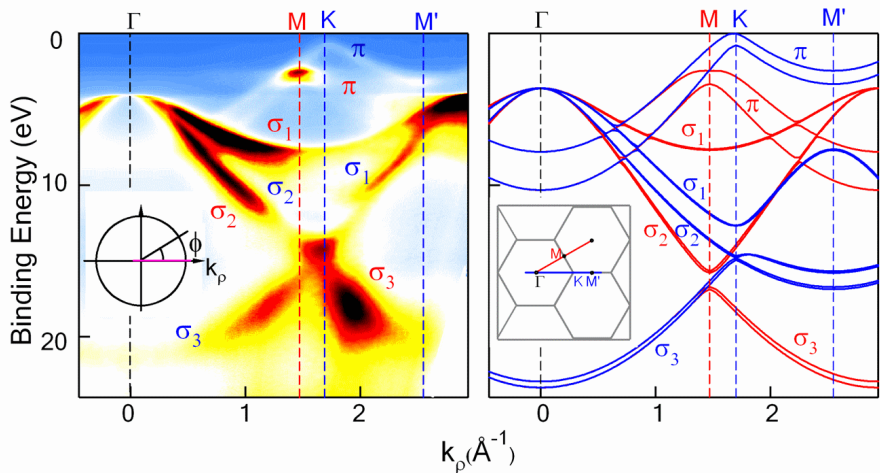
- 1 Motivation
- 2 Angle Resolved Photoelectron Spectroscopy
 - Introduction and Basic Principle
 - Energy Relations and Analysis
 - Design of an Energy Analyser
- 3 Zero Gap Semiconductor
 - Survey in Gray Tin
 - Alloys of CdTe and HgTe
- 4 Measurements and Results
 - Preparation
 - Measurement Results
- 5 Summary and Outlook
 - Summary
 - Outlook

Bandstructure and Fermi Surface

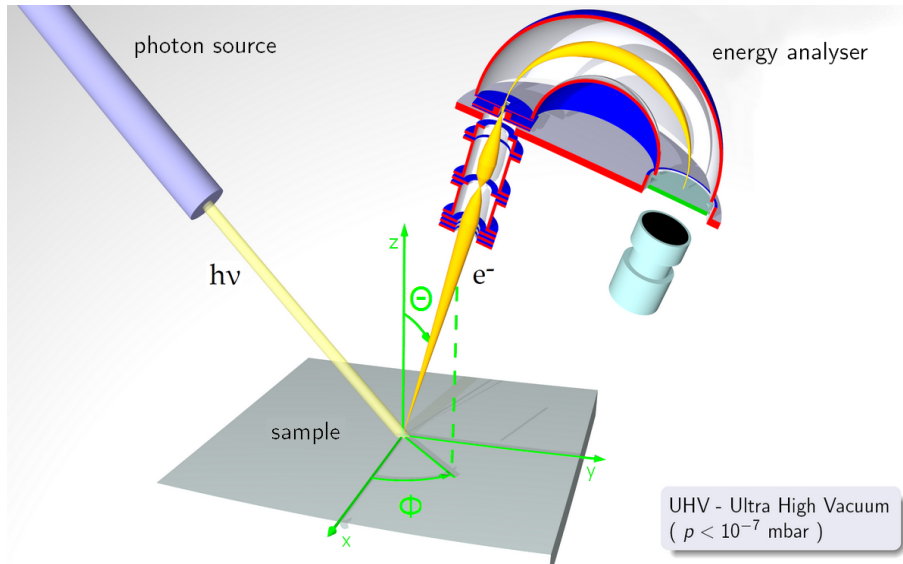


Experimental Results vs. Theory

Photo Electron Spectroscopy on Graphite



General Setup



Step 1: Photoexcitation of the Electron

Transition Propability

The probability ω_{fi} of the transition for an electron from initial state $|\Phi_i\rangle$ to final state $|\Phi_f\rangle$ is given by Fermis Golden Rule:

$$\omega_{fi} = \frac{2\pi}{\hbar} |\langle \Phi_f | H_{WW} | \Phi_i \rangle|^2 \delta(E_f - E_i - \hbar\omega)$$

Step 1: Photoexcitation of the Electron

Transition Propability

The probability ω_{fi} of the transition for an electron from initial state $|\Phi_i\rangle$ to final state $|\Phi_f\rangle$ is given by Fermis Golden Rule:

$$\omega_{fi} = \frac{2\pi}{\hbar} |\langle \Phi_f | H_{WW} | \Phi_i \rangle|^2 \delta(E_f - E_i - \hbar\omega)$$

Hamiltonian

The interaction between electron and photon is described by the Hamiltonian H_{WW} . In Coulomb gauge and linear approximation it is

$$H_{WW} = \frac{e}{2mc} \vec{A} \cdot \vec{p}$$

Step 1: Photoexcitation of the Electron

Transition Propability

The probability ω_{fi} of the transition for an electron from initial state $|\Phi_i\rangle$ to final state $|\Phi_f\rangle$ is given by Fermis Golden Rule:

$$\omega_{fi} = \frac{2\pi}{\hbar} |\langle \Phi_f | H_{WW} | \Phi_i \rangle|^2 \delta(E_f - E_i - \hbar\omega)$$

Hamiltonian

The interaction between electron and photon is described by the Hamiltonian H_{WW} . In Coulomb gauge and linear approximation it is

$$H_{WW} = \frac{e}{2mc} \vec{A} \cdot \vec{p}$$

Energy Konservation

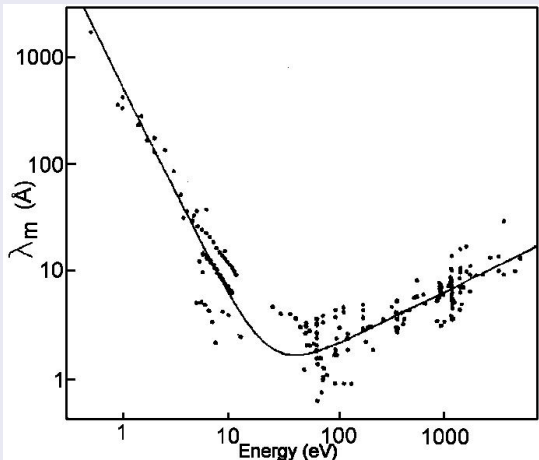
$$E_f = E_i + \hbar\omega$$

Momentum Konservation

$$\vec{k}_i = \vec{k}_f$$

Step 2: Transport to the Surface

Mean Free Electron Path in Bulk Material



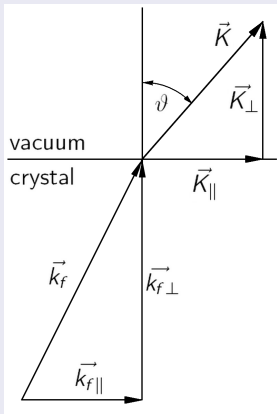
Limiting Step

At UV excitation energies the mean free path is merely 10 Å. One has to care about surface states, clean surfaces that represent bulk material and UHV conditions. Surface sensitivity can be used for band deflection by controlled adsorption.

Secondaries

By scattering a spectra of low energy secondary electrons is generated.

Step 3: Penetration through the surface



\vec{K} wave vector in vakuum,
 \vec{k}_f is wave vector of the
 final state in crystal

Dispersion of free Electron

Excited bulk state interacts with free electron state:

$$E_{kin} = \frac{\hbar^2}{2m_e} \vec{K}^2$$

Refraction of Electrons at Surface

Parallel component (plus lattice vector \vec{g}_{\parallel}):

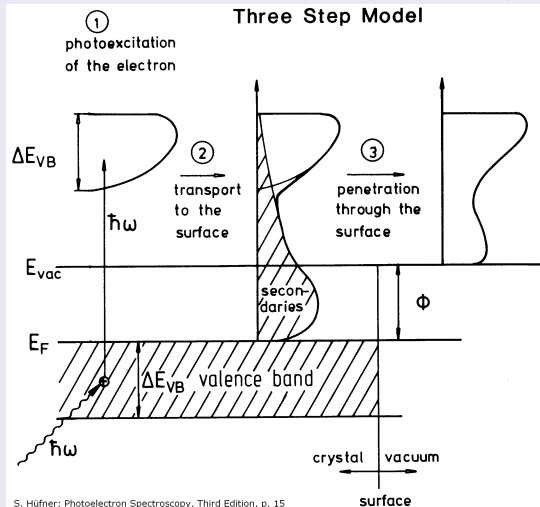
$$\vec{k}_{i\parallel} = \vec{k}_{f\parallel} = \vec{K}_{\parallel} = \sqrt{\frac{2m}{\hbar}} E_{kin} \sin \vartheta$$

Final state energy and perpendicular component:

$$E_f = \frac{\hbar^2}{2m} (\vec{k}_f + \vec{G})^2 - |V_0|$$

$$k_{f\perp} = \sqrt{\frac{2m}{\hbar^2} (E_{kin} + |V_0|) - \vec{G}_{\parallel}^2 - G_{\perp}} \quad \vartheta = 0$$

Energy Relations during Measuring Process



Kinetic Energy

$$E_{kin} = \frac{\vec{p}^2}{2m_e} = \frac{m_e}{2} \vec{v}^2$$

Lorentz Force

$$\vec{F} = q(\vec{E} + \vec{v} \times \vec{B})$$

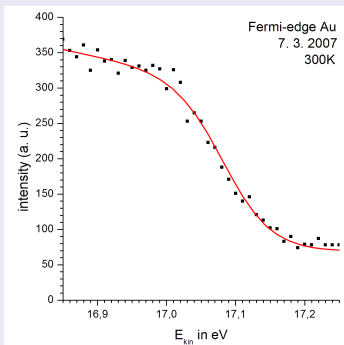
$$B \leq 0.25 \mu T$$

Example

$\hbar\omega$	=	21.2eV	He-I
Φ	=	4.8eV	Au
E_{kin}	=	16.4eV	E_F

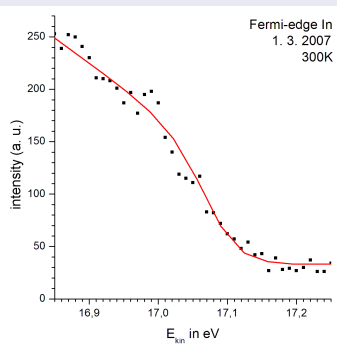
Invariance of measured Fermi-Energy on Work Function

Fermi-edge Gold, $\Phi = 4.8$ eV



$$E_F = (17.085 \pm 0.004) \text{ eV}$$

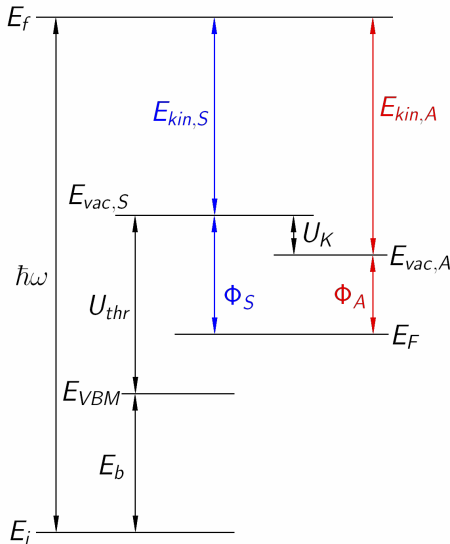
Fermi-edge Indium, $\Phi = 4.12$ eV



$$E_F = (17.076 \pm 0.005) \text{ eV}$$

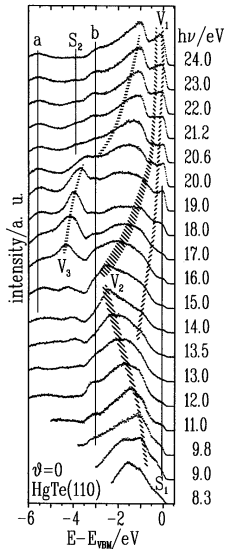
The measured Fermi-energy does not depend on the work function of the sample. During the measuring process the entire spectrum is shifted.

Work Function and Energy Relations

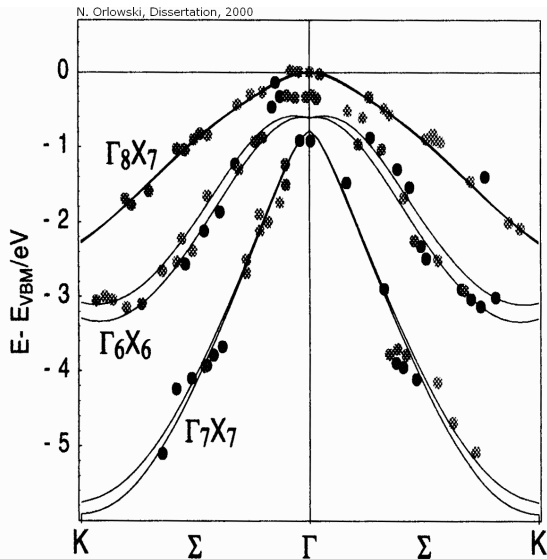
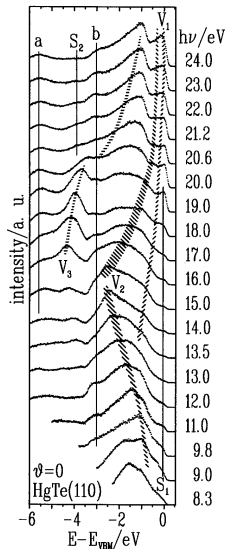


- E_i energy of initial state
- E_f energy of final state
- E_{VBM} valence band maximum
- $E_{vac,S}$ vacuum level of sample
- $E_{vac,A}$ vacuum level of analyser
- $\hbar\omega$ photon energy
- U_b binding energy
- E_{thr} threshold of photo emission
- $E_{kin,S}$ kinetic energy of electrons at the sample
- $E_{kin,A}$ kinetic energy of electrons at analyser
- U_K contact potential
- Φ_S work function of sample
- Φ_A work function of analyser
- E_F Fermi energy

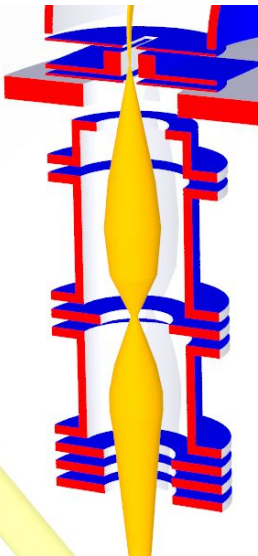
Fitting and resulting Band Structure



Fitting and resulting Band Structure



Retarding and Focussing



Preretarding stage

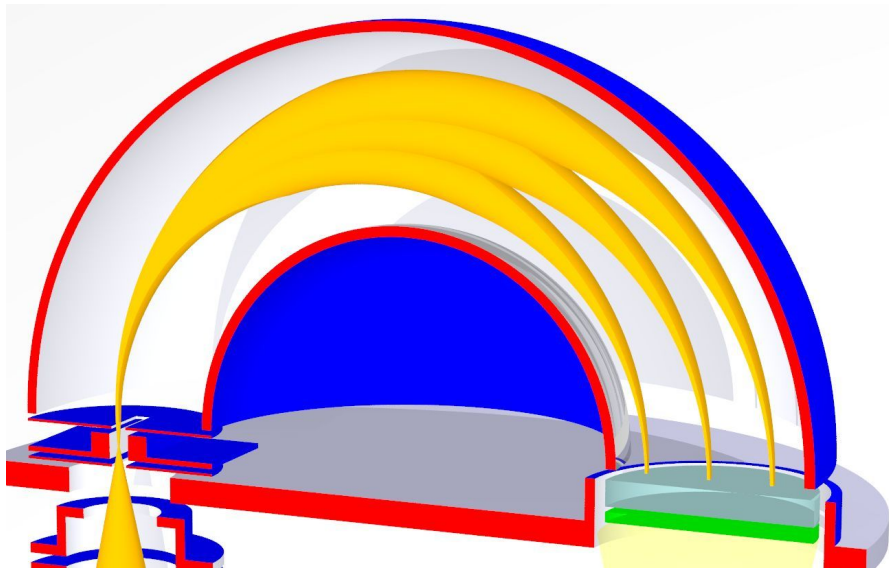
Usually a preretarding stage is used prior to the energy analysis. Electrons enter the analyser with a specified pass energy. One can decelerate (or accelerate) electrons (almost) without changing their absolute energy spread. Measured kinetic energy:

$$E_{kin,A} = E_{pass} - U_{ret}$$

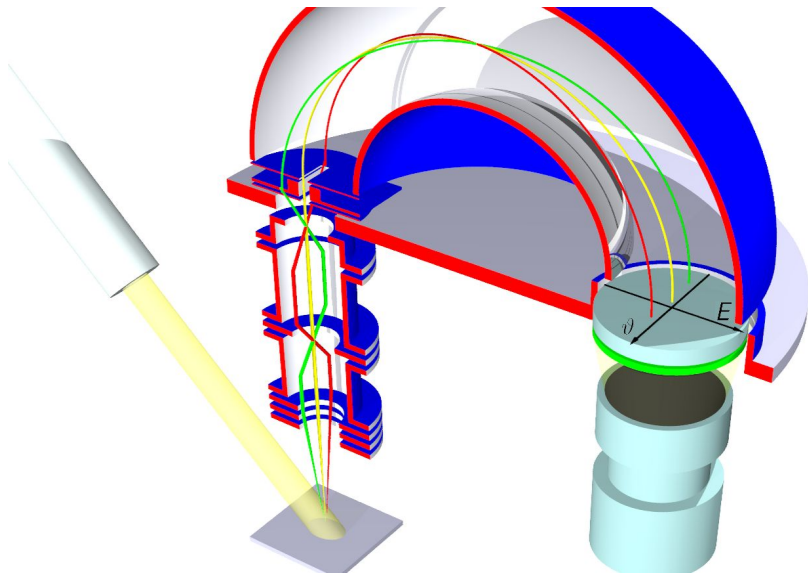
Negative Kinetic Energy

$E_{kin,S}$	=	0.2 eV
U_{ret}	=	10.2 eV
U_K	=	-0.4 eV
E_{pass}	=	10 eV
$E_{kin,A}$	=	-0.2 eV

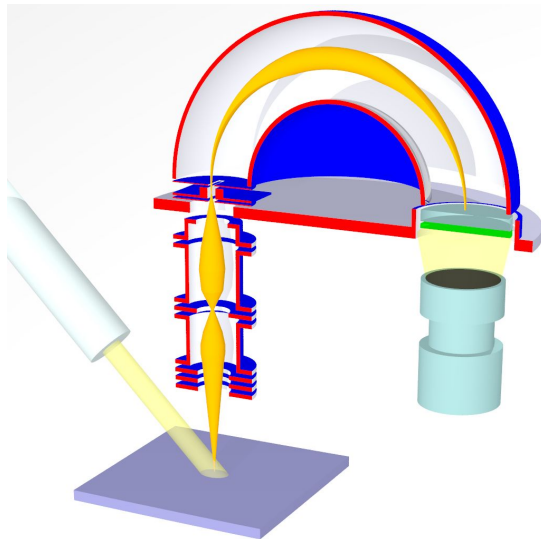
Energy Dispersion inside Spherical Condensator



Angle Resolution by Mapping of Entrance Point



Resolution of Spherical Analyser



Potentials on hemispheres

For transmission of electrons with initial energy E_0 along a path with $R_0 = (R_{in} + R_{out})/2$ the potential has to be

$$V_{out} = E_0[3 - 2(R_0/R_{out})]$$

$$V_{in} = E_0[3 - 2(R_0/R_{in})]$$

Resolution

$$\frac{\Delta E}{E_{pass}} = \frac{w}{2R_0} + \alpha^2$$

w width entrance slit
 α acceptance angle

Survey of Narrow-Gap Semiconductors: α -Sn

- (I) crucial magnetoresistance measurements on n-type material by Ewald's group which showed no anisotropy at 4 or 77 K but a dominance of electrons of (111) symmetry at 200 K
- (II) measurements of conductivity, Hall effect and susceptibility at temperatures above 150 K, which demonstrated an activation energy of 0.08 eV
- (III) measurement of an electron mass of $0.02 m_0$ which was inconsistent with a small ($\Gamma_8^+ - \Gamma_7^-$) gap
- (IV) pressure measurements which gave a high-temperature pressure coefficient consistent with conduction band minima at the L point
- (V) pressure measurements on conductivity and Hall effect at low temperatures which were inconsistent with the presence of (111) electrons and also of (000) electrons in a Γ_7^- extremum

No conventional positive-gap band structure could fit all of these criteria.

William Paul & Steven Groves: *Band Structure of Gray Tin*, 1963, Phys. Rev. Lett. **11** 194

Inverted Bandstructure

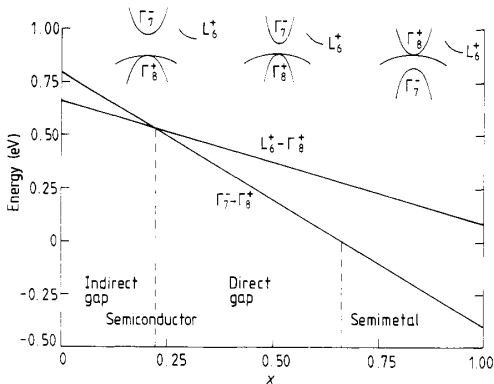


Figure 1. Variation of the energy differences ($\Gamma_7^- - \Gamma_8^+$) and $L_6^+ - \Gamma_8^+$) in the alloy system $\text{Ge}_{1-x}\text{Sn}_x$. For $x = 0$, the smallest band gap ($L_6^+ - \Gamma_8^+$) is indirect, with a value of about 0.65 eV at room temperature; the direct gap ($\Gamma_7^- - \Gamma_8^+$) is about 0.8 eV. For $x = 1$, the indirect gap ($L_6^+ - \Gamma_8^+$) is ~ 0.1 eV and the direct gap ($\Gamma_7^- - \Gamma_8^+$) about -0.4 eV.

α -Sn paper

Results for HgTe was in S. Groves thesis, but statement about it was taken out of *PRL* paper in case speculations on this material they had not measured themselves would jeopardise publication.

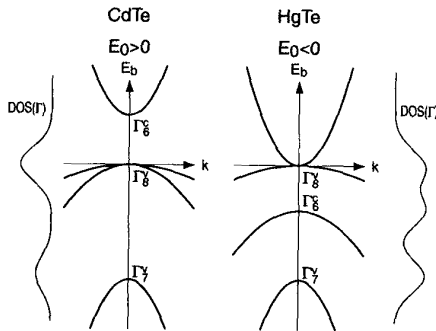
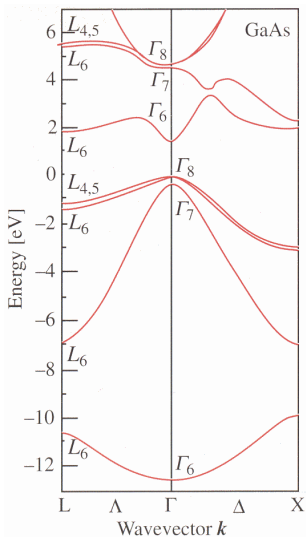
ZnS semiconductors

bandgap definition:

$$E_0 = E(\Gamma_6) - E(\Gamma_8)$$

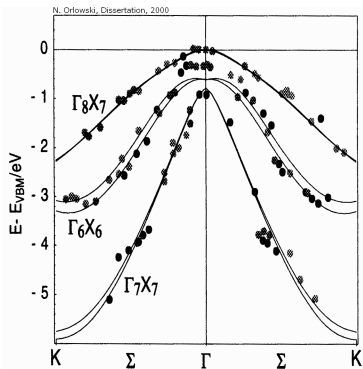
(direct bandgap)

Bandgap for CdTe, HgTe and $\text{Cd}_x\text{Hg}_{1-x}\text{Te}$



CdTe	property	HgTe
0,675	Phillips-Van Vechten ionicity f_i	0,68
6.488	lattice constant	6.445
1.56	gap	-0.283

$\text{Cd}_x\text{Hg}_{1-x}\text{Te}$



inverted bandstructure of HgTe,
measured with ARPES

Properties

CdTe and HgTe are consolute. The bandgap can be free adjusted. The alloys have a high electron mobility and a high optic absorption coefficient.

Fabrication

- modified Bridgeman technique
- molecular beam epitaxy (MBE)

Application

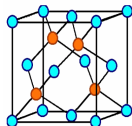
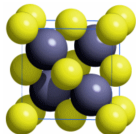
- dual-band infrared detectors with high quantum efficiency (simultaneous detection in the MWIR and LWIR)
- CCD-array for IR-astronomy

Samples of $\text{Cd}_x\text{Hg}_{1-x}\text{Te}$

Ia	Ib	II	IIIa
			
			
x=0,07	x=0,07	x=0,4	x=0,2
127,0 mg		130,3 mg	91,6 mg
<111>	<111>		<110>
			
			
x=0,2	x=0,183	x=0,1955	x=0,1046
66,9 mg	129,2 mg	248,5 mg	108,9 mg
<110>	<110>	<110>	<110>

Data of Samples

Nr.	X	weight
Ia	0,07	127 mg
Ib	0,07	
II	0,4	130 mg
IIIa	0,2	92 mg
IIIb	0,2	67 mg
IV	0,183	129 mg
V	0,1955	248 mg
VI	0,105	109 mg



Crystal Quality - Laue Images

Polaroid and Simulation



Image generated with LauePT 2.1 (programm for Laue Pattern, programmed by XianRong Huang, Stony Brook University, Southampton; www.sunysb.edu)

10KV 40mA 12h
verkippt: 

Sample Ib

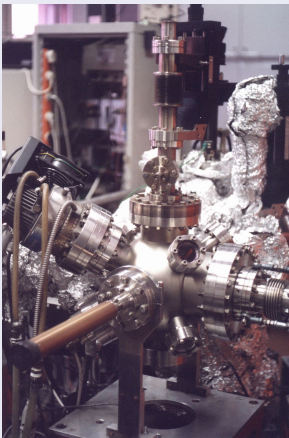
$\text{Cd}_{0.07}\text{Hg}_{0.93}\text{Te}$



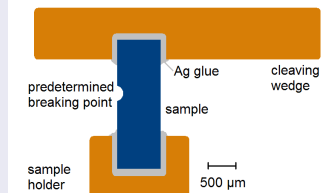
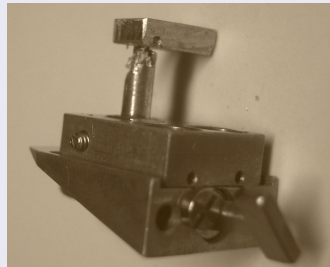
thickness: 620 μm

weight: 81 mg

Surface Preparation - Cleavage Mechanism



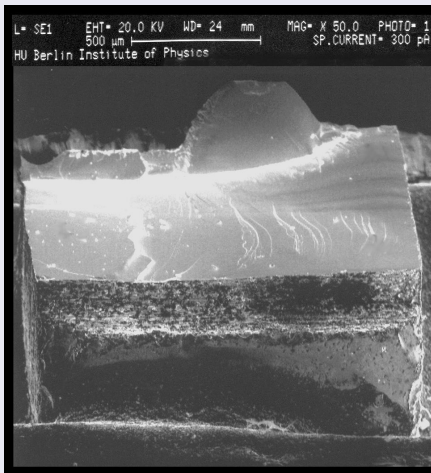
cleavage chamber by
N. Orlowski, assembled 2000



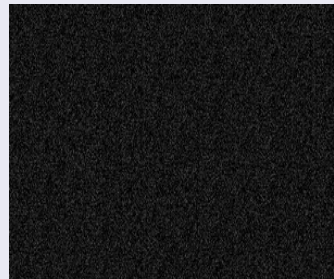
cleavage in sample holder

Surface Quality after Cleavage

SEM Image

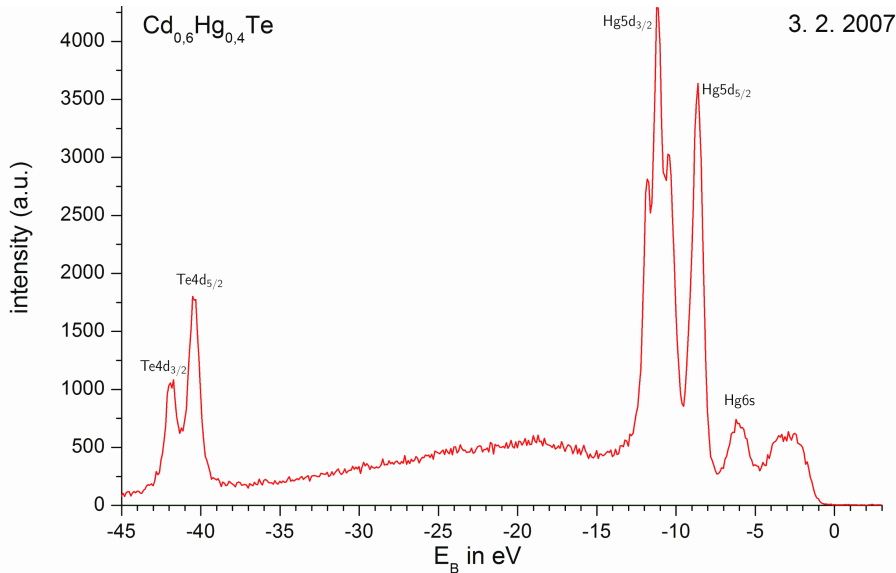


LEED Image



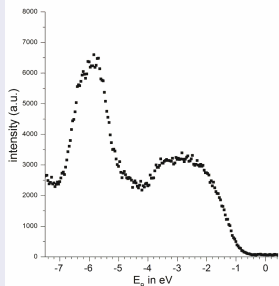
Reasons for LEED

- craggedness of cleavage
- spot size electron beam
- failure in apparatus

BESSY Measurements at BUS Beamline, $\hbar\omega = 80$ eV

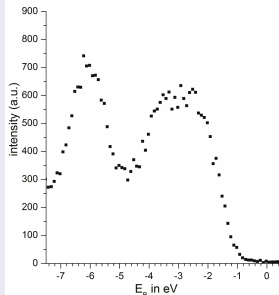
Dispersion in Valence Band? Gap? Peak Position?

BESSY $h\nu = 40$ eV



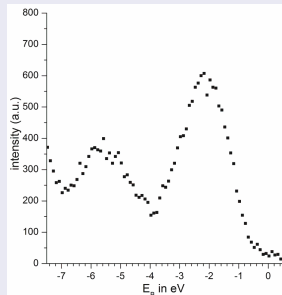
$\text{Cd}_{0.18}\text{Hg}_{0.82}\text{Te}$
26. 1. 2007

BESSY $h\nu = 80$ eV



$\text{Cd}_{0.4}\text{Hg}_{0.6}\text{Te}$
3. 2. 2007

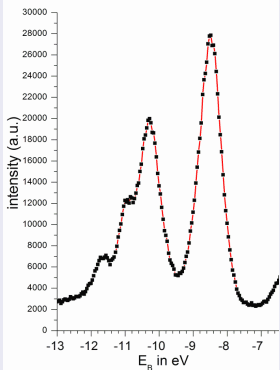
He-I $h\nu = 21.2$ eV



$\text{Cd}_{0.2}\text{Hg}_{0.8}\text{Te}$
8. 3. 2007

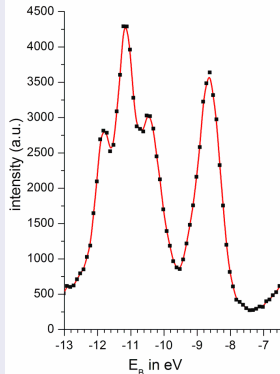
Cleavage Quality - Satellites of $Hg5d_{3/2}$

BESSY $h\nu = 40$ eV



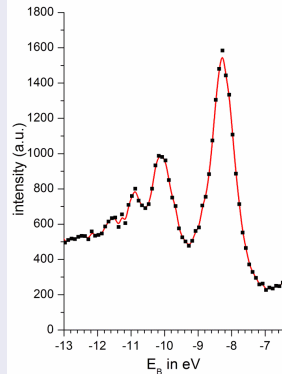
$Cd_{0.18}Hg_{0.82}Te$
26. 1. 2007

BESSY $h\nu = 80$ eV



$Cd_{0.4}Hg_{0.6}Te$
3. 2. 2007

He-I $h\nu = 21.2$ eV



$Cd_{0.2}Hg_{0.8}Te$
8. 3. 2007

X. Yu, L. Vanzetti, G. Haugstad, A. Raisanen, A. Franciosi: *Inequivalent sites for Hg at the HgTe (110) surface*. Surf. Sci **275**, 92-100, (1992)

Conclusion

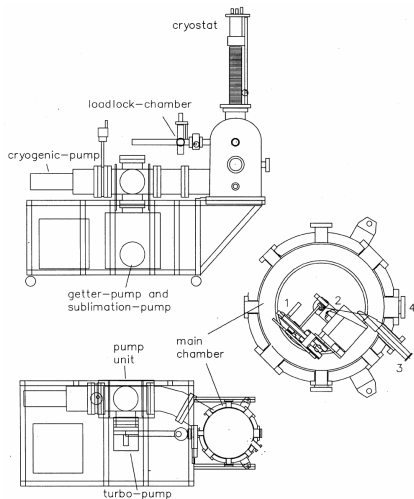


Photo Electron Spectroscopy

- powerful technique to determine bandstructure and electronic properties of solids
- detected electrons easy to analyse
- surface sensitive
- UHV conditions inevitable

Conclusion

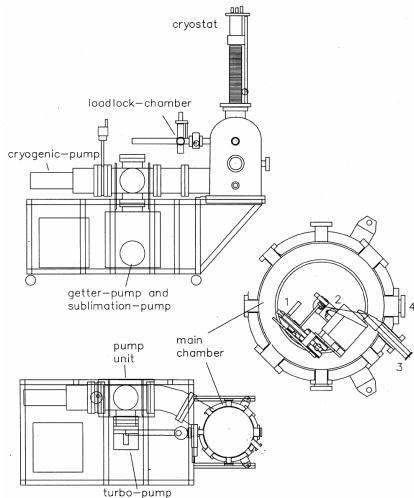


Photo Electron Spectroscopy

- powerful technique to determine bandstructure and electronic properties of solids
- detected electrons easy to analyse
- surface sensitive
- UHV conditions inevitable

$\text{Cd}_x\text{Hg}_{1-x}\text{Te}$

- first angle resolved measurement
- inverted bandstructure - zero gap
- complicated (110) surface preparation

Outlook

Measurement

- Laue pictures of measured crystals
- LEED at WESPHOA chamber
- EDX for composition
- automatic nitrogen refill system
- measurements at BESSY training beamline with synchrotron light and new Scienta
- cooled cleavage

More Samples ...

- samples of already grown $\text{Cd}_x\text{Hg}_{1-x}\text{Te}$ crystals from Hr. Sölle
- growth of new $\text{Pb}_x\text{Zn}_{1-x}\text{Te}$
- more samples from Moscow



Thanks for your attention!